

NASNet: A Neuron Attention Stage-by-Stage Net for Single Image Deraining

Xu Qin

School of Electronics Engineering and Computer Science, Peking University

qinxu@pku.edu.cn

Zhilin Wang

School of Computer Science and Engineering, Beihang University

007wangzhilin@buaa.edu.cn

Abstract

Images captured under complicated rain conditions often suffer from noticeable degradation of visibility. The rain models generally introduce diversity visibility degradation, which includes rain streak, rain drop as well as rain mist. Numerous existing single image deraining methods focus on the only one type rain model, which does not have strong generalization ability. In this paper, we propose a novel end-to-end Neuron Attention Stage-by-Stage Net (NASNet), which can solve all types of rain model tasks efficiently. For one thing, we pay more attention on the Neuron relationship and propose a lightweight Neuron Attention (NA) architectural mechanism. It can adaptively recalibrate neuron-wise feature responses by modelling interdependencies and mutual influence between neurons. Our NA architecture consists of Depthwise Conv and Pointwise Conv, which has slight computation cost and higher performance than SE block by our contrasted experiments. For another, we propose a stage-by-stage unified pattern network architecture, the stage-by-stage strategy guides the later stage by incorporating the useful information in previous stage. We concatenate and fuse stage-level information dynamically by NA module. Extensive experiments demonstrate that our proposed NASNet significantly outperforms the state-of-the-art methods by a large margin in terms of both quantitative and qualitative measures on all six public large-scale datasets for three rain model tasks.

1. Introduction

Images taken under complicated rainy condition often contain some of undesired artifacts, which can severely affect the human visual perceptual assessment and the performance of the high-level computer vision tasks, e.g., person re-identification [37], visual tracking [24][23], object detection [7]. In the past decades, we have witnessed more and

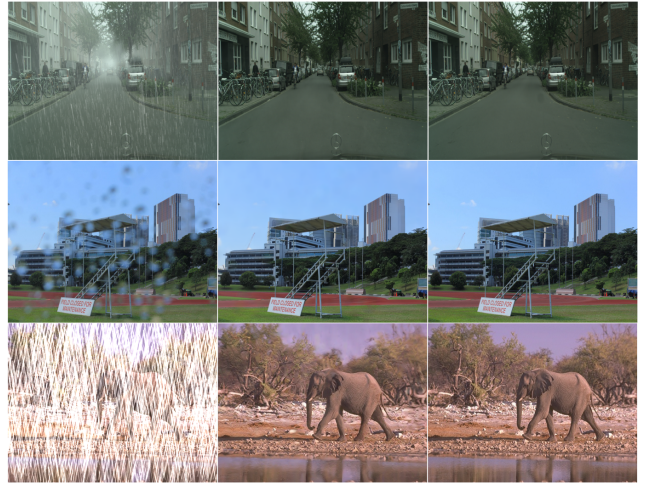


Figure 1. The rain mist, rain drop and rain streak model examples. The first column is the rain image, the second column is our NASNet outputs, the last column is the ground truth.

more researchers develop various algorithms in single image deraining. Early deraining methods focus on the image priors methods [33, 15, 3, 42, 1, 12, 20]. With the rising-up of the deep learning technology, lots of CNN-based models [38, 11, 17, 41, 18, 35, 30, 5] have been proposed. There are usually three major rain model categories: raindrop, rain streak, as well as rain mist.

Although these state-of-the-art methods can produce reasonable results on different rain model datasets, the main limitation of these algorithms is that they are specially designed to deal with certain rain model task on certain dataset. Referring to [17], most of their methods does not have a good generalization ability and network capacity, which is reflected in the fact that they do not achieve satisfactory results when applied to other rain removal tasks. For example, rain streak removal methods apply to rain drop task in Section 4.3. In this paper, we focus on automatically generating sharp rain-free image from a rainy input, and

propose a Neuron Attention Stage-by-Stage Net for single image deraining which can cope with all above rain models.

The emergence of ResNet [8] makes it possible to build larger and larger networks which imposes a significant increase in model complexity. The contradiction is that lightweight network deployment on the mobile side is an inevitable trend. Furthermore, since the attention [34, 43, 32] as a mechanism to recalibrate the informative components has been widely used in plenty of AI tasks. To solve the above questions, we propose an efficient and lightweight attention structure rather than simply stacking network layers based on the original network to improve the network capacity and flexibility. It can explicitly model the interdependencies between the neurons of convolutional features in network, through which our NA combining the spatial information in each channel and the depth information in each space to selectively emphasize the informative neurons rather than unimportant ones. As we all know, convolutional filters can fuse channel-wise and spatial-wise relationship together within local receptive fields to combine the structure information in last convolutional features. Consequently, the output after the convolution is unable to exploit contextual information outside of the local region in the last layer of convolution.

From NA, we recalibrate the value of each neuron response and value by fusing the information of peripheral neurons. Meanwhile, the peripheral neurons correspond to their local receptive field information in the last convolutional features. Consequently, it breaks the limitation that the response of this neuron can only obtain information from the last convolutional local receptive fields.

It has been proved by Hu et al.'s [10] that the benefits of attention mechanism can be accumulated through the entire network whether it is in the early layers to share low-level representations or in the later layers to response specialized tasks. We significantly improve the network's representation capacity by stacking a series of NA structures in our NASNet to perform dynamic Neuron-wise information recalibration. And extensive experiments also demonstrate that our NA has slight computation cost and higher performance than SE block [10]. Because of the complexity of three rain models, we decided to make most of multiple stages pattern to design our network, while adding stage-level feature concatenation and fusion structure by dynamically recalibrating neuron-wise response. The previous stage's information can guide the later stages' study and enable redundant information to go to deep layers without too much processing. Ablation experiments show that stage-level feature concatenation and adaptive recalibration bring out huge performance improvement.

It has been demonstrated by Lim et al.'s [21] that stacked residual blocks, skip connections and Local Residual Learning can be used to construct high-performance CNN. Con-

sequently, Our NASNet with Global Residual Learning contains multiple stages, each stage with long skip connection combines a number of blocks, each block with Local Residual Learning consists of many convolution operations with short skip connection, adaptive and dynamic recalibration by NA.

By adopting NASNet, we achieve the best results on six datasets for three rain model tasks. Experiments demonstrate that our NASNet outperforms previous state-of-the-art methods both quantitatively and qualitatively. The ablation experiments and component analysis confirm our network architecture's efficiency and necessity.

1.1. Our Contribution

Main contributions of our paper are listed as follows:

- We propose an end-to-end Neuron Attention Stage-by-Stage Net (NASNet) for single image deraining, NASNet has excellent network capacity and generalization ability than those who can only deal with certain rain model on certain dataset. It outperforms previous state-of-the-art algorithms on all six public large-scale datasets and rain streak, rain drop as well as rain mist models.
- We propose a lightweight but novel neuron attention (NA) structure. Our NA can adaptively recalibrate neuron-wise feature response by dynamically modeling the interdependencies of neurons. It has less computation cost, breaks the limitation of local receptive fields in last layers, achieves the remarkable results while imposing only a slight network burden.
- We propose a stage-by-stage pattern architecture while adding the stage-level features concatenation and dynamic fusion module by recalibrating the neuron-wise response. The result shows this architecture can cope with three complex rain models, ablation experiments also demonstrate that both stage-by-stage pattern and stage-level feature concatenation module can bring out huge performance improvement.
- We make most of the network-level Global Residual Learning, Stage-level Long Skip Connection, block-level Local Residual Learning, and convolution-level short skip connection, adaptive and dynamic recalibration. By combining these operations, the performance of our NASNet is further improved.

2. Related work

2.1. Single Image Deraining Methods

Prior-based algorithms. Early prior-based methods have been proposed to deal with rain image by designing hand-crafted priors based on statistics to solve these

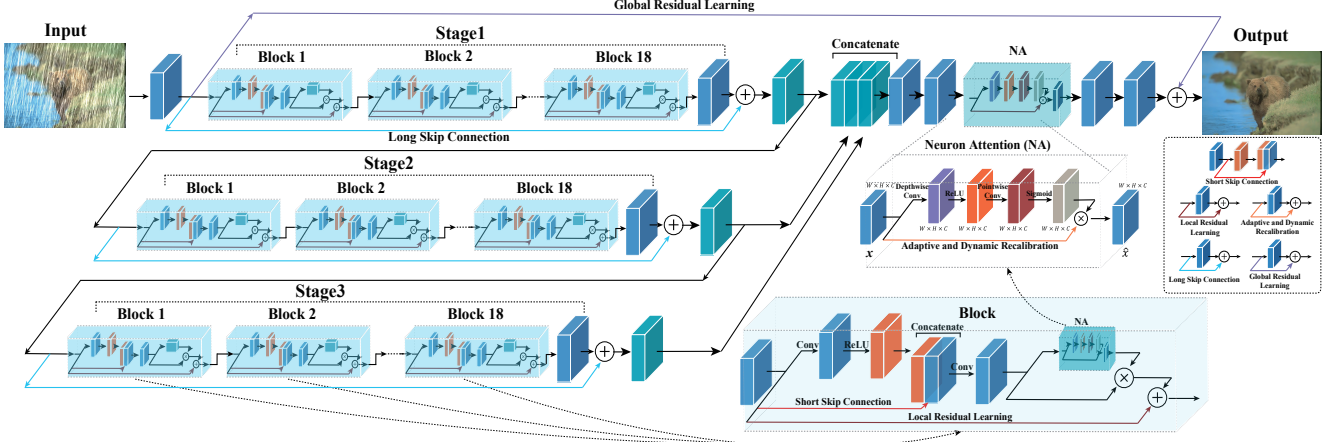


Figure 2. The neuron attention stage-by-stage net (NASNet) architecture.

problems. For example, sparse coding-based methods [44, 15, 20], low-rank representation-based methods [3, 40]. GMM-based (Gaussian Mixture Model) model [19] to separate the streak layer, have achieved the satisfactory result. However, these prior-based methods limit the capacity to remove the rain, they can not recover the high-frequency texture background and image details [15, 40].

CNN-based algorithms. With big data driven and computing power greatly improved, CNN-based algorithms have achieved immense success in almost all computer vision tasks including single image deraining [18, 17, 16, 39]. Yang et al.’s [38] develop a multi-task deep learning architecture that learns the binary rain streak map. Fu et al.’s [5] use a prior image domain knowledge by focusing on high frequency detail during training, which removes background interference and focuses the model on the structure of rain in images. Zhang et al.’s [41] propose method enables the network itself to automatically determine the rain-density information and then efficiently remove the corresponding rain-streaks guided by the estimated rain density label. Ren et al.’s [31] provide a simpler baseline deraining network by considering network architecture, input and output, and loss functions.

CNN with attention mechanism algorithms. Attention can be viewed as a tool or mechanism to process the most important components of input signals [13, 14, 26]. The attention mechanism achieved dominant success in image deraining task. Qian et al.’s [30] apply an attentive generative network using adversarial training, their main idea is to inject visual attention into both the generative and discriminative networks. Li et al.’s [18] assign different alpha-values to various rain streak layers according to the intensity and transparency by incorporating the squeeze-and-excitation block. Hu et al.’s [11] design an end-to-end deep neural network, where they train it to learn depth-attentional features via a depth-guided attention mechanism. Wang et al.’s

[35] propose spatial attentive residual blocks to remove rain streaks in a local-to-global manner.

2.2. Rain Models

Taking the rain density, wind velocity, raindrop size factors into consideration, rain can introduce a few types of visibility degradation. Most of previous works focus on rain streak removal task, it can not cover all rain model problems obviously. We divide the rain model into three categories: rain streak, raindrop and rain mist.

Rain streak. Rain streak image R_s can be viewed as the composition of the rain-free background scene B and the line-shape rain streak layer S :

$$R_s = B + S \quad (1)$$

Rain streaks can occlude and reduce the visibility of the background scene. We can obtain the clear image B by removing the streak layer S .

Rain drop. Raindrops D attached to camera lens, window glass will obstruct, deform the clean background scenes B , thereby forming a Rain drop image R_d .

$$R_d = (1 - M) \odot B + D \quad (2)$$

where M is a binary mask and \odot means element-wise multiplication. $M(x) = 1$, if a pixel x belong to raindrop region, and otherwise means it is a part of background. The goal is to obtain the rain-free image B from a given input R_d .

Rain mist. Distant rain streaks S accumulate and produce atmospheric veiling effects in a manner more like haze or mist phenomenon R_m . This situation often occurs in real outdoor rain scenes. The presence of Rain mist will greatly affect the visibility of objects and scene in the captured rain-free image B . Based on the atmosphere scattering model [28, 2, 29], it is modeled as the blow formulation:

$$R_m = B \odot t + A(1 - t) + S \quad (3)$$

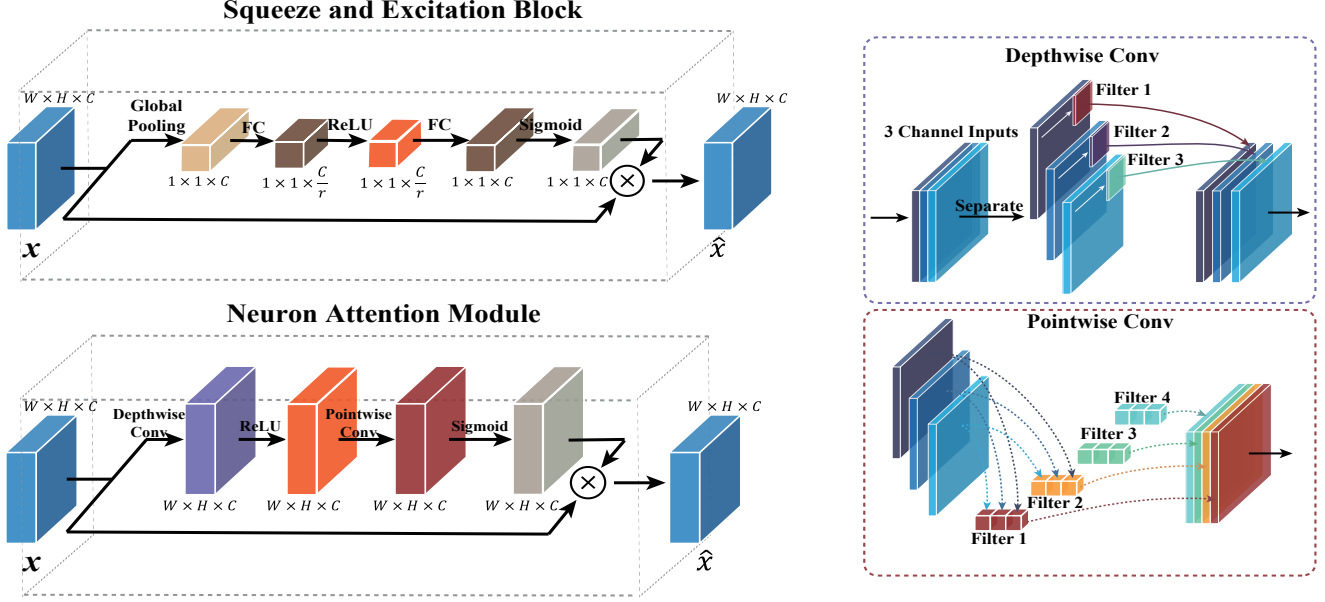


Figure 3. The architecture comparison between SE block and our proposed NA.

where t and A are the transmission map and global atmospheric light in atmosphere scattering model. These two parameters can determine the presence and concentration of mist. We are committed to solving the problem of the combination of rain and mist.

3. Proposed model

We propose an end-to-end NASNet to remove rain artifacts in a stage-by-stage manner, as shown in Fig.2. The whole architecture consist of a stage-by-stage unified architecture, we make most of the network-level Global Residual Learning, stage-level Long Skip Connection, block-level Local Residual Learning, and convolution-level short skip connection, adaptive and dynamic recalibration.

3.1. Neuron Attention (NA)

Our proposed NA module in Fig.3 is lightweight but novel, it is committed to greatly improving the sensitivity of information processing compared with other conventional networks. In this way, we can focus more attention on valuable neurons or features, which can be explored in the subsequent convolution operation. NA can adaptively and dynamically recalibrate neuron-wise response by modelling interdependencies and mutual influence between neurons, which mainly relies on two operations, depthwise convolution and pointwise convolution.

Depthwise Convolution. We use depthwise convolution (upper right of Fig.3) to make full use of the spatial information in each channel. Depthwise Convolution is completed in a two-dimensional plane, and the number of filter is the same as the depth of the last layer. After the depthwise con-

volution, we apply a simple gate mechanism ReLU activation [27] to realize nonlinearity property. These operations can be formulated as:

$$Y_c = \delta(W_d(X_c)) \quad (4)$$

where δ denotes the ReLU activation function, c denotes c -th feature, W_d is the weight set of a depthwise convolution operation. Y_c stands for the middle output of the c -th feature.

Pointwise Convolution. In order to tackle the issue of that Depthwise Convolution can not effectively utilize the information of different maps in the same spatial location, we then adopt the Pointwise Convolution operation (bottom right of Fig.3), whose convolution kernel size is 1×1 , where depth denotes the number of feature map of last layer. The final output of Pointwise Convolution is obtained by employing a sigmoid activation function. These operations can be formulated as:

$$\hat{X} = \sigma(W_p(Y)) \quad (5)$$

The σ denotes the sigmoid activation function. \hat{X} denotes the final result, and W_p stands for the weight set of a pointwise convolution operation.

The extensive experiments and component analysis prove that NA can achieve remarkable results while imposing only a slight network burden.

3.2. Stage-by-Stage Unified Pattern Architecture

Considering the complexity of rain models, we specifically designed our network structure in a stage-by-stage

unified pattern to better remove rain artifacts from the input. Our whole network contains three stage structure, each stage with long skip connection combining multiple blocks, each block with Local Residual Learning consisting of many convolution operations with short skip connection, adaptive and dynamic recalibration. At last, we add a Global Residual Learning operation and a stage-level features concatenation and dynamic fusion structure.

The stage-by-stage strategy can guide the later stage by incorporating the useful information in the previous stage, selectively handling more important information, making the redundant information go to deep layer without too much processing.

Ablation experiments and component analysis show that Stage-by-Stage architecture and stage-level feature concatenation can bring out huge performance improvement.

3.3. Loss Function

We minimize the following joint loss function L to train our NASNet:

$$L_{total} = L_1 + L_{SSIM} \quad (6)$$

The L_{SSIM} can be expressed as:

$$L_{SSIM} = 1 - SSIM(pred, gt) \quad (7)$$

Where $pred$ is the predicted result and gt is the rain-free image. We use the standard L_1 loss to measure the per-pixel reconstruction accuracy rather than L_2 loss according to [21]. L_{SSIM} [36] has also been widely adopted in image restoration tasks [6]. L_{SSIM} indicates the structural similarities between the output and clear image.

4. Experiments

4.1. Training Settings

In the training process, we use a batch size of two with the crop size of 240×240 , we augment data by randomly rotate 90,180,270 degrees and horizontal flip. The number of feature map is 64, and the kernel size is 3×3 . The initial learning rate is 2×10^{-4} , RAdam [22] optimization algorithm is used, the parameters take default value. Cosine annealing strategy [9] is adopted to adjust it. The entire network is trained for up to 3×10^5 iterations using PyTorch framework with two RTX 2080Ti GPUs.

4.2. Metrics

We evaluate the performance of different image deraining methods on six public large-scale datasets and three rain model tasks. The widely used peak-signal-to-noise-ratio (PSNR) and structure similarity index (SSIM) metrics are adopted to quantify output image quality. We also provide a comparison of the output images for human subjective assessment.

4.3. Datasets and Experimental Results

In this section, we will introduce some public large-scale datasets that appear in the experimental section and compare NASNet metrics with previous state-of-the-art image deraining methods both quantitatively and qualitatively. These methods include DDN [5], JORDER [38], DID-MDN [41], DerainDropGAN [30], RESCAN [18], DAF-Net [11], SPANet [35], PReNet [31].

As more and more researchers pay attention to the rain removal task, plenty of deraining datasets are proposed. These large-scale datasets undoubtedly promote the development of the rain removal field. The previous works mainly focused on the synthetic rain streak removal datasets. Recently, a series of real world rain datasets or rain drop, rain mist datasets are published in succession.

4.3.1 Rain100L and Rain100H image datasets

(1)**Rain100L** is the synthetic dataset with only one type of rain streak. (2)**Rain100H** is the synthetic dataset with five streak directions. The images for Rain100H and Rain100L are selected from BSD200 [25] proposed by Yang et al. 's [38]. The specific quantitative comparisons on **Rain100H** can be seen in table 1.

Methods	PSNR	SSIM
JORDER	22.15	0.6736
JORDER-R	23.45	0.7490
DDN	21.92	0.7640
DID-MDN	25.00	0.7543
RESCAN	26.45	0.8458
DAF-Net	28.44	0.8740
PReNet	<u>29.46</u>	<u>0.8990</u>
Ours	30.38	0.9252

Table 1. Quantitative comparisons on Rain100H dataset for different methods.

Because of the simplicity of the Rain100L dataset, we only compare the latest state-of-the-art methods.

Methods	PSNR	SSIM
DDN	32.16	0.9360
JORDER	36.11	0.9700
PReNet	<u>37.48</u>	<u>0.9790</u>
Ours	39.55	0.9880

Table 2. Quantitative comparisons on Rain100L dataset for different methods.

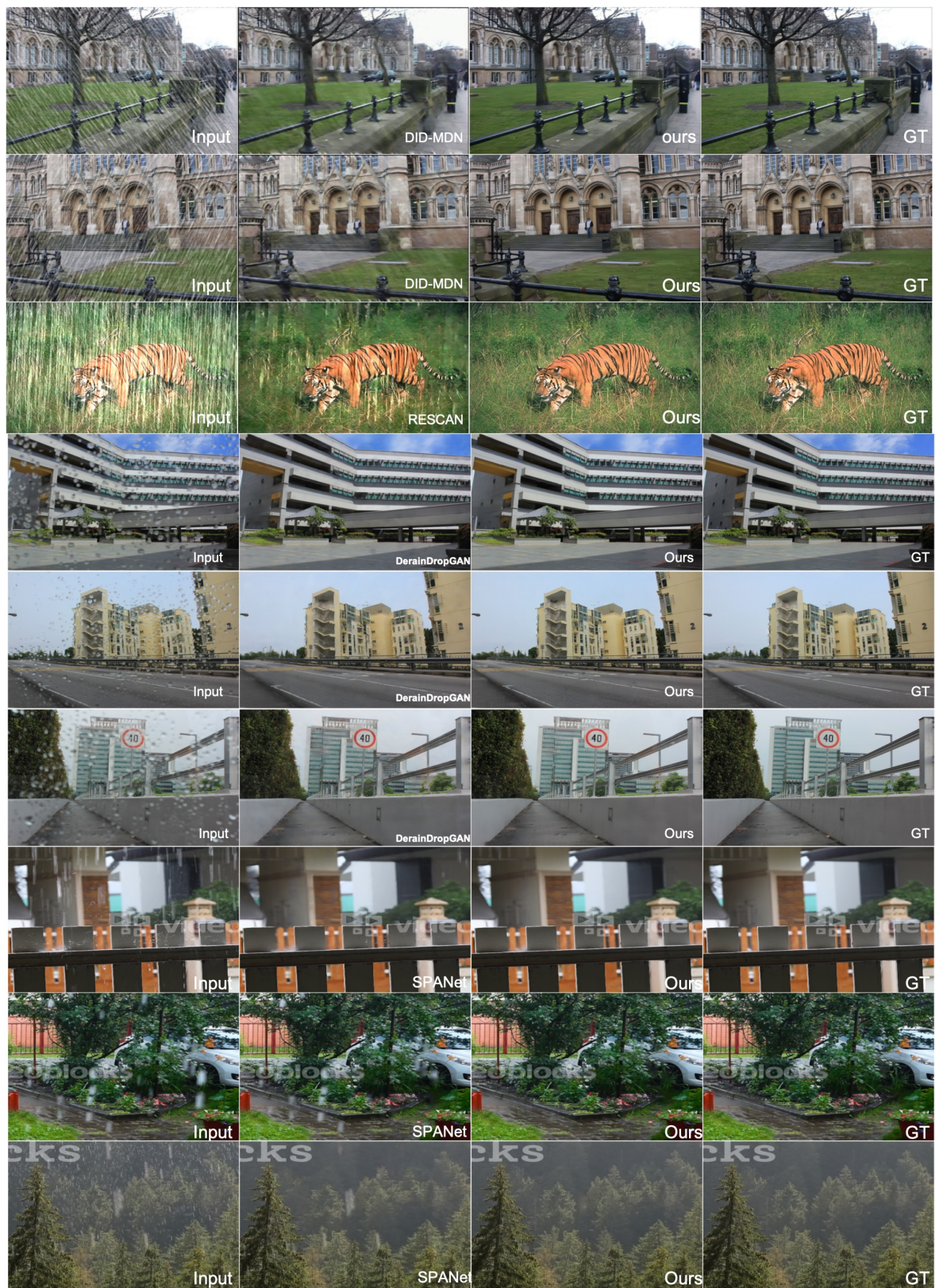


Figure 4. The qualitative comparisons of different methods on synthetic and real rain image datasets. More image output results can be seen in supplementary material.

4.3.2 SPA-REAL dataset

The author did not name the (3)SPA-REAL dataset, SPA-REAL is named after ourselves. Wang et al. [35] construct a large-scale dataset of 29.5K real rain/rain-free image pairs that covers a wide range of natural rain scenes using 170 real rain videos, of which 84 scenes are captured by using iPhone X or iPhone6SP and 86 scenes are collected from StoryBlocks or YouTube. The author split into 28,500 for training and 1,000 for testing. We have also obtained experimental results on SPA-REAL in table 3.

Methods	PSNR	SSIM
JORDER	35.72	0.9776
DDN	34.88	0.9727
DID-MDN	28.96	0.9457
RESCAN	35.19	0.9784
SPA	38.06	0.9867
Ours	43.50	0.9879

Table 3. Quantitative comparisons on SPA-REAL dataset for different methods.

4.3.3 RainCityScapes dataset

(4)RainCityScapes is released by Hu et al.’s [11] with rain streaks and fog, they adopt the outdoor photos in the Cityscapes dataset [4] as their rain-free image, and utilize the camera parameters and depth information in the Cityscapes dataset to synthesize rain and fog on the photos. their dataset has 9,432 training images and 1,188 test images. From table.4, we can see the comparison results on RainCityScapes.

Methods	PSNR	SSIM
DID-MDN	28.43	0.9349
RESCAN	24.49	0.8852
DAF-Net	30.06	0.9530
Ours	34.79	0.9888

Table 4. Quantitative comparisons on RainCityScapes dataset for different methods.

4.3.4 MPID datasets

(5)MPID-drop), (6)MPID-streak and (7)MPID-mist are released by Li et al. ’s [17]. They include both synthetic and real-world images. However, the number of image pairs mentioned in the paper does not correspond to the number of open sources. We abandon the rain mist dataset. The results among different methods can be seen in table 5.

PSNR/SSIM \ Datasets	MPID-drop	MPID-streak
Methods		
JORDER	27.52 / 0.8239	26.26 / 0.8089
DDN	25.23 / 0.8336	29.39 / 0.7854
DID-MDN	24.76 / 0.7930	26.80 / 0.8028
DerainDropGAN	31.57 / 0.9023	- / -
Ours	30.75 / 0.9255	30.64 / 0.8911

Table 5. Quantitative comparisons on MPID-streak and MPID-drop datasets for different methods.

4.3.5 Qualitative Comparisons

Besides the PSNR, SSIM objective metrics, we conduct the human assessment for subjective evaluation. We further provide a large amount of output image comparisons. The visual comparisons of our NASNet with previous state-of-the-art methods are in Fig. 4. The first six rows’ rain streak and rain drop results are conducted on the synthesized datasets, including Rain100H, MPID-streak, MPID-drop. We can clearly see that our results are very close to the real natural scene. DID-MDN[41], RESCAN [18] can’t completely remove the rain streak. The Derain-DropGAN deforms and twists in some high-frequency areas such as the lower-right corner road in row4, the stairs and junctions in the middle building in row 5 and the windows at the left side of the building in row 6, DerainDropGAN is also unsatisfactory in the performance of color fidelity. The last three rows are on the real rain image dataset SPA-REAL. Our results remove the rain artifacts almost entirely, and they are more similar to rain-free images. Compared with SPANet, our NASNet achieves the remarkable performance, SPANet can clearly see the existence of raindrops and rain streak.

5. Ablation Study and Component Analysis

5.1. Neuron Attention (NA) Analysis

We mainly analyze the lightness and efficiency of our NA module.

Lightness: The lightness of our NA module is revealed in the fact that the sum of the parameters of Depthwise Convolution and Pointwise Convolution is about one third of the parameters of default convolution operation. Hu et al.’ [10] squeeze-and-excitation (SE) block is a commonly used and popular attention block. We compare the parameters of SE block with our NA module in different settings, as shown in Fig.5, where k stands for kernel size, reduction denotes feature map reducing to $1/reduction$ in the middle operation. Furthermore, our NASNet’s total parameters are

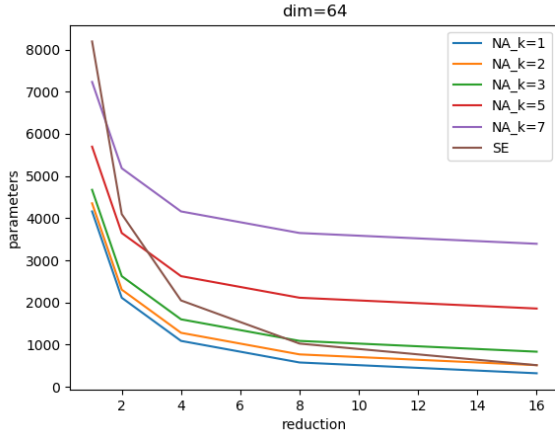


Figure 5. The parameters comparison of squeeze-and-excitation block with our NA module with 64 feature maps.

6, 508, 931. It will reduce to 6, 244, 931, if we remove all NA module. Consequently, we can draw a full conclusion that our NA will impose slight network burden.

Architecture	Total parameters
NASNet	6, 508, 931
NASNet without NA	6, 244, 931

Table 6. The total parameters comparison of NASNet and NASNet without NA.

Efficiency: To prove our NA has higher and remarkable performance than SE block, we replace the NA module with SE block (SENet) or remove all attention module (PlainNet), and keep other structures unchanged. We conduct contrasted experiments on SPA-REAL dataset with initial learning rate 1×10^{-4} and 2×10^5 steps.

Network Architecture	PSNR	SSIM
PlainNet	40.85	0.9841
SENet	40.93	0.9838
NASNet	41.1373	0.9843

Table 7. Network performance comparison according to different attention architecture. PlainNet stands for removing the attention block from NASNet.

From the table.7 results, we can see that the attention mechanism can improve the network flexibility and capacity. Our NA achieves more remarkable performance than SENet.

5.2. Stage-by-Stage Pattern Analysis

In this section, we will analyze the effectiveness of our Stage-by-Stage pattern architecture with the last concatenation and fusion module by NA. Specifically, we set the

number of stage to 1, 2, 3, 4 to compare their network performance respectively. We conduct our experiments on the Rain100H dataset, the specific PSNR/SSIM metrics can be seen in the table.8.

Stages numbers	PSNR	SSIM
Stage=1	28.9818	0.9077
Stage=2	29.7786	0.9170
Stage=3	30.3777	0.9252
Stage=4	30.4611	0.9257

Table 8. Network performance comparison according to different number of stages.

From the table, we can easily find out that the network performance improves gradually with the increase of the number of stages. When the number of stages changes from 3 to 4, the performance improvement is not so obvious. However, the larger number of stages costs more training time and consumes more computing resources. As a trade-off, we use stages=3 for our NASNet network.

5.3. Stage-level Information Concatenation and Fusion

In order to further analyze the efficiency of every component of our network structure, we ultimately conduct ablation experiments on the concatenation and fusion module. The experiments are training and testing on the SPA-REAL dataset with initial learning rate $1 \times e^{-4}$ and $2 \times e^5$ steps, one net is NASNet, the other is DirectNet (that is, without stage-level information concatenation and fusion module). The comparison results are as follows:

Architecture	PSNR	SSIM
DirectNet	40.9513	0.9840
NASNet	41.1373	0.9843

Table 9. The performance comparison of NASNet and DirectNet, DirectNet stands for removing stage-level information concatenation and fusion module from NASNet.

The comparison results show that concatenation and fusion module can bring out performance result. It enhances the NASNet’s capacity.

6. Conclusion

This paper proposes an end-to-end Neuron Attention Stage-by-Stage Net (NASNet) for single image deraining. It has excellent generalization, which can achieve remarkable results on six public datasets for three rain models. Our proposed lightweight but novel NA module can adaptively and dynamically recalibrate neuron-wise response, we believe that NA can still play an important role in different

field tasks. Our stage-by-stage pattern architecture can provide more thinking and reference for solving rain removal or other field problems. The ablation experiments and component analysis also prove that our structure has their own efficiency and necessity. Finally, we are curious to explore the contribution of our NA in other image processing fields.

References

- [1] Jérémie Bossu, Nicolas Hautière, and Jean-Philippe Tarel. Rain or snow detection in image sequences through use of a histogram of orientation of streaks. *International journal of computer vision*, 93(3):348–367, 2011. **1**
- [2] Earl J Cartney. Optics of the atmosphere: scattering by molecules and particles. *New York, John Wiley and Sons, Inc.*, 1976. 421 p., 1976. **3**
- [3] Yi-Lei Chen and Chiou-Ting Hsu. A generalized low-rank appearance model for spatio-temporally correlated rain streaks. In *Proceedings of the IEEE International Conference on Computer Vision*, pages 1968–1975, 2013. **1, 3**
- [4] Marius Cordts, Mohamed Omran, Sebastian Ramos, Timo Rehfeld, Markus Enzweiler, Rodrigo Benenson, Uwe Franke, Stefan Roth, and Bernt Schiele. The cityscapes dataset for semantic urban scene understanding. In *Proceedings of the IEEE conference on computer vision and pattern recognition*, pages 3213–3223, 2016. **7**
- [5] Xueyang Fu, Jiabin Huang, Delu Zeng, Yue Huang, Xinghao Ding, and John Paisley. Removing rain from single images via a deep detail network. In *Proceedings of the IEEE Conference on Computer Vision and Pattern Recognition*, pages 3855–3863, 2017. **1, 3, 5**
- [6] Xueyang Fu, Borong Liang, Yue Huang, Xinghao Ding, and John Paisley. Lightweight pyramid networks for image deraining. *IEEE transactions on neural networks and learning systems*, 2019. **5**
- [7] Ross Girshick. Fast r-cnn. In *Proceedings of the IEEE international conference on computer vision*, pages 1440–1448, 2015. **1**
- [8] Kaiming He, Xiangyu Zhang, Shaoqing Ren, and Jian Sun. Deep residual learning for image recognition. In *Proceedings of the IEEE conference on computer vision and pattern recognition*, pages 770–778, 2016. **2**
- [9] Tong He, Zhi Zhang, Hang Zhang, Zhongyue Zhang, Junyuan Xie, and Mu Li. Bag of tricks for image classification with convolutional neural networks. In *Proceedings of the IEEE Conference on Computer Vision and Pattern Recognition*, pages 558–567, 2019. **5**
- [10] Jie Hu, Li Shen, and Gang Sun. Squeeze-and-excitation networks. In *Proceedings of the IEEE conference on computer vision and pattern recognition*, pages 7132–7141, 2018. **2, 7**
- [11] Xiaowei Hu, Chi-Wing Fu, Lei Zhu, and Pheng-Ann Heng. Depth-attentional features for single-image rain removal. In *Proceedings of the IEEE Conference on Computer Vision and Pattern Recognition*, pages 8022–8031, 2019. **1, 3, 5, 7**
- [12] De-An Huang, Li-Wei Kang, Yu-Chiang Frank Wang, and Chia-Wen Lin. Self-learning based image decomposition with applications to single image denoising. *IEEE Transactions on multimedia*, 16(1):83–93, 2013. **1**
- [13] Laurent Itti and Christof Koch. Computational modelling of visual attention. *Nature reviews neuroscience*, 2(3):194, 2001. **3**
- [14] Laurent Itti, Christof Koch, and Ernst Niebur. A model of saliency-based visual attention for rapid scene analysis. *IEEE Transactions on Pattern Analysis & Machine Intelligence*, (11):1254–1259, 1998. **3**
- [15] Li-Wei Kang, Chia-Wen Lin, and Yu-Hsiang Fu. Automatic single-image-based rain streaks removal via image decomposition. *IEEE Transactions on Image Processing*, 21(4):1742–1755, 2011. **1, 3**
- [16] Ruoteng Li, Loong-Fah Cheong, and Robby T Tan. Heavy rain image restoration: Integrating physics model and conditional adversarial learning. In *Proceedings of the IEEE Conference on Computer Vision and Pattern Recognition*, pages 1633–1642, 2019. **3**
- [17] Siyuan Li, Iago Breno Araujo, Wenqi Ren, Zhangyang Wang, Eric K Tokuda, Roberto Hirata Junior, Roberto Cesar-Junior, Jiawan Zhang, Xiaojie Guo, and Xiaochun Cao. Single image deraining: A comprehensive benchmark analysis. In *Proceedings of the IEEE Conference on Computer Vision and Pattern Recognition*, pages 3838–3847, 2019. **1, 3, 7**
- [18] Xia Li, Jianlong Wu, Zhouchen Lin, Hong Liu, and Hongbin Zha. Recurrent squeeze-and-excitation context aggregation net for single image deraining. In *Proceedings of the European Conference on Computer Vision (ECCV)*, pages 254–269, 2018. **1, 3, 5, 7**
- [19] Yu Li and Michael S Brown. Single image layer separation using relative smoothness. In *Proceedings of the IEEE Conference on Computer Vision and Pattern Recognition*, pages 2752–2759, 2014. **3**
- [20] Yu Li, Robby T Tan, Xiaojie Guo, Jiangbo Lu, and Michael S Brown. Rain streak removal using layer priors. In *Proceedings of the IEEE conference on computer vision and pattern recognition*, pages 2736–2744, 2016. **1, 3**
- [21] Bee Lim, Sanghyun Son, Heewon Kim, Seungjun Nah, and Kyoung Mu Lee. Enhanced deep residual networks for single image super-resolution. In *Proceedings of the IEEE conference on computer vision and pattern recognition workshops*, pages 136–144, 2017. **2, 5**
- [22] Liyuan Liu, Haoming Jiang, Pengcheng He, Weizhu Chen, Xiaodong Liu, Jianfeng Gao, and Jiawei Han. On the variance of the adaptive learning rate and beyond. *arXiv preprint arXiv:1908.03265*, 2019. **5**
- [23] Cong Ma, Yuan Li, Fan Yang, Ziwei Zhang, Yueqing Zhuang, Huizhu Jia, and Xiaodong Xie. Deep association: End-to-end graph-based learning for multiple object tracking with conv-graph neural network. In *Proceedings of the 2019 on International Conference on Multimedia Retrieval*, pages 253–261. ACM, 2019. **1**
- [24] Cong Ma, Changshui Yang, Fan Yang, Yueqing Zhuang, Ziwei Zhang, Huizhu Jia, and Xiaodong Xie. Trajectory factory: Tracklet cleaving and re-connection by deep siamese bi-gru for multiple object tracking. In *2018 IEEE International Conference on Multimedia and Expo (ICME)*, pages 1–6. IEEE, 2018. **1**

- [25] David Martin, Charless Fowlkes, Doron Tal, Jitendra Malik, et al. A database of human segmented natural images and its application to evaluating segmentation algorithms and measuring ecological statistics. *Iccv Vancouver*., 2001. 5
- [26] Volodymyr Mnih, Nicolas Heess, Alex Graves, et al. Recurrent models of visual attention. In *Advances in neural information processing systems*, pages 2204–2212, 2014. 3
- [27] Vinod Nair and Geoffrey E Hinton. Rectified linear units improve restricted boltzmann machines. In *Proceedings of the 27th international conference on machine learning (ICML-10)*, pages 807–814, 2010. 4
- [28] Srinivasa G Narasimhan and Shree K Nayar. Chromatic framework for vision in bad weather. In *Proceedings IEEE Conference on Computer Vision and Pattern Recognition. CVPR 2000 (Cat. No. PR00662)*, volume 1, pages 598–605. IEEE, 2000. 3
- [29] Srinivasa G Narasimhan and Shree K Nayar. Vision and the atmosphere. *International journal of computer vision*, 48(3):233–254, 2002. 3
- [30] Rui Qian, Robby T Tan, Wenhan Yang, Jiajun Su, and Jiaying Liu. Attentive generative adversarial network for rain-drop removal from a single image. In *Proceedings of the IEEE Conference on Computer Vision and Pattern Recognition*, pages 2482–2491, 2018. 1, 3, 5
- [31] Dongwei Ren, Wangmeng Zuo, Qinghua Hu, Pengfei Zhu, and Deyu Meng. Progressive image deraining networks: a better and simpler baseline. In *Proceedings of the IEEE Conference on Computer Vision and Pattern Recognition*, pages 3937–3946, 2019. 3, 5
- [32] Masanori Suganuma, Xing Liu, and Takayuki Okatani. Attention-based adaptive selection of operations for image restoration in the presence of unknown combined distortions. In *Proceedings of the IEEE Conference on Computer Vision and Pattern Recognition*, pages 9039–9048, 2019. 2
- [33] Shao-Hua Sun, Shang-Pu Fan, and Yu-Chiang Frank Wang. Exploiting image structural similarity for single image rain removal. In *2014 IEEE International Conference on Image Processing (ICIP)*, pages 4482–4486. IEEE, 2014. 1
- [34] Ashish Vaswani, Noam Shazeer, Niki Parmar, Jakob Uszkoreit, Llion Jones, Aidan N Gomez, Łukasz Kaiser, and Illia Polosukhin. Attention is all you need. In *Advances in neural information processing systems*, pages 5998–6008, 2017. 2
- [35] Tianyu Wang, Xin Yang, Ke Xu, Shaozhe Chen, Qiang Zhang, and Rynson WH Lau. Spatial attentive single-image deraining with a high quality real rain dataset. In *Proceedings of the IEEE Conference on Computer Vision and Pattern Recognition*, pages 12270–12279, 2019. 1, 3, 5, 7
- [36] Zhou Wang, Alan C Bovik, Hamid R Sheikh, Eero P Simoncelli, et al. Image quality assessment: from error visibility to structural similarity. *IEEE transactions on image processing*, 13(4):600–612, 2004. 5
- [37] Fan Yang, Ke Yan, Shijian Lu, Huizhu Jia, Xiaodong Xie, and Wen Gao. Attention driven person re-identification. *Pattern Recognition*, 86:143 – 155, 2019. 1
- [38] Wenhan Yang, Robby T Tan, Jiashi Feng, Jiaying Liu, Zongming Guo, and Shuicheng Yan. Deep joint rain detection and removal from a single image. In *Proceedings of the IEEE Conference on Computer Vision and Pattern Recognition*, pages 1357–1366, 2017. 1, 3, 5
- [39] Rajeev Yasarla and Vishal M Patel. Uncertainty guided multi-scale residual learning-using a cycle spinning cnn for single image de-raining. *arXiv preprint arXiv:1906.11129*, 2019. 3
- [40] He Zhang and Vishal M Patel. Convolutional sparse and low-rank coding-based rain streak removal. In *2017 IEEE Winter Conference on Applications of Computer Vision (WACV)*, pages 1259–1267. IEEE, 2017. 3
- [41] He Zhang and Vishal M Patel. Density-aware single image de-raining using a multi-stream dense network. In *Proceedings of the IEEE conference on computer vision and pattern recognition*, pages 695–704, 2018. 1, 3, 5, 7
- [42] Xiaopeng Zhang, Hao Li, Yingyi Qi, Wee Kheng Leow, and Teck Khim Ng. Rain removal in video by combining temporal and chromatic properties. In *2006 IEEE International Conference on Multimedia and Expo*, pages 461–464. IEEE, 2006. 1
- [43] Yulun Zhang, Kunpeng Li, Kai Li, Lichen Wang, Bineng Zhong, and Yun Fu. Image super-resolution using very deep residual channel attention networks. In *Proceedings of the European Conference on Computer Vision (ECCV)*, pages 286–301, 2018. 2
- [44] Lei Zhu, Chi-Wing Fu, Dani Lischinski, and Pheng-Ann Heng. Joint bi-layer optimization for single-image rain streak removal. In *Proceedings of the IEEE international conference on computer vision*, pages 2526–2534, 2017. 3